Coalescence of drops on the free-surface of a liquid pool at elevated temperatures

Pavan Kumar Kirar[a], Kathryn Alvarenga[b], Pankaj Kolhe[c], Gautam Biswas[d], Kirti Chandra Sahu[a,*]

[a] *Department of Chemical Engineering, Indian Institute of Technology Hyderabad, Sangareddy 502 285, Telangana, India*
[b] *Department of Aerospace Engineering, Texas A&M University, College Station, TX, 77843-3141, USA*
[c] *Department of Mechanical and Aerospace Engineering, Indian Institute of Technology Hyderabad, Sangareddy 502 285, Telangana, India*
[d] *Department of Mechanical Engineering, Indian Institute of Technology Kanpur, Kanpur - 208016, India*

Abstract

The coalescence dynamics of ethanol drops injected from a needle on the free-surface of an ethanol pool maintained at a higher temperature than the drop is experimentally studied using a high-speed imaging system. The drop is always kept at 25°C and the temperature of the ethanol pool is varied using a heater. The coalescence behavior depends on the size of the drop, the height of the needle tip from the free-surface and the temperature of the ethanol pool. A parametric study is carried out by varying these parameters. The drop exhibits a residence period at low impact velocity, when it floats on the free-surface before the coalescence begins. Subsequently, the complete coalescence and partial coalescence dynamics are observed for different sets of parameters considered. It is found that increasing the temperature of the ethanol pool reduces the residence time of the drop. This phenomenon is explained by analyzing the forces acting on the drop and the capillary waves generated due to the temperature gradient between the drop and the ethanol pool. During partial coalescence, we also observed that the diameter of the daughter droplet decreases as the size of the primary drop and pool temperature are increased. As expected, due to the gravity effect, increasing the size of the drop also decreases the residence time. A regime map designating the complete coalescence and partial coalescence dynamics is plotted in the pool temperature and drop impact height space.

---

[*] Corresponding author
Email address: `ksahu@che.iith.ac.in` (Kirti Chandra Sahu)

Preprint submitted to Physics of Fluids *April 19, 2020*

Nomenclature

Symbol	Description
σ	Surface tension
ΔT	Temperature difference between the drop and pool
T_s	Temperature at the free-surface of an ethanol pool
t_r	Residence time of the drop
t_c	Time scale of thermal diffusion
τ	Dimensionless time, t/t_c
τ_r	Dimensionless residence time, t_r/t_c
Ma	Marangoni number
D_p	Diameter of the primary drop
D_s	Diameter of the daughter droplet
H	Height of the needle tip from the ethanol-air interface
h	Height of the bottom of the drop from the ethanol-air interface
μ_l	Dynamic viscosity of ethanol
ρ_l	Density of ethanol
ρ_a	Density of air
ν	Kinematic viscosity of air
α	Thermal diffusivity of ethanol
U	Impact velocity of the drop
W	Weight of the drop
F_b	Buoyancy force
F_l	Surface tension force
A	Surface area the curved surface
r_c	Radius the curved surface

1. Introduction

The impact of a drop on the solid or free-surface of a liquid pool has fascinated researchers for many decades because of its importance in a wide range of applications, including microfluidics, combustion, coatings, inkjet printing, soil erosion or air trapping on the sea surface, to name a few (see, for instance, Refs.[1–5]). Drop coalescence on a heated liquid pool can also be observed in several practical applications, such as bioprinting, oil industry, production of nanoparticles, and microfluidic technologies [6–9]. As in the present study, we focus on the dynamics of a drop slowly placed on the free-surface of a liquid pool maintained at different temperatures, we only review the literature concerned with the collision of the drop with a liquid-air interface. A drop falling in a liquid pool undergoes various regimes as the impact velocity increases, such as spreading, partial coalescence and splashing [10]. Despite a large volume of work conducted for the isothermal system (when the drop and the liquid pool are at the same temperature; see, for instance, Refs. [11–18]), the non-isothermal system (when the drop and the liquid pool are at different temperatures and thermocapillary stresses can play an important role; see Ref. [19]) has received far less attention in the literature.

When a small liquid drop comes into contact with a free-surface of a liquid pool in an isothermal environment, the drop undergoes either spreading as it drains completely inside the pool or undergoes partial coalescence dynamics as a satellite drop pinches off depending on its impacting velocity and size, as well as the fluid properties of the liquids [20]. At low impact velocity, the primary drop injected from a needle floats on the free-surface while the trapped air between the drop and the free-surface drains out. In reaction, the air film of decreasing thickness generates a lubrication force that balances the droplet weight. This period when drop floats on the surface is termed as the 'residence time' [14, 21, 22]. Subsequently, the drop comes in contact with the free-surface at a point and due to high capillary pressure, it undergoes rapid spreading. This in turn generates upward-moving capillary waves that form a liquid column. At this stage, the surface tension (σ) squeezed the bottom of the liquid column which experiences a competition between the vertical and horizontal collapses due to upward moving capillary waves and the surface tension force, respectively. Under certain conditions, the horizontal collapse overcomes the vertical collapse, and the liquid column is detached from free-surface as a daughter drop of diameter about half of the primary drop [14, 17]. The daughter drops completely drains in the liquid pool, under a coalescence cascading cycle. Originally, partial coalescence was thought to be a result of an inviscid instability [11] but later it was found to be regulated mainly by gravity, viscosity, and interfacial stress [12, 14]. Couder *et al.* [23] have demonstrated that with a silicone oil of kinematic viscosity 500 cSt, the critical acceleration of bouncing drop increases as the square of the frequency of oscillation of the surface. We note a similarity with the inelastic bouncing ball model since small drops deform the bath weakly. All the above-mentioned studies are conducted in isothermal environment. Considering the Marangoni flow resulting from the surfactant gradient, Haldar *et al.* [24] reported that the number of coalescence cascading cycles decreases as the surfactant concentration increases.

In non-isothermal configuration, few researchers [25–27] investigated experimentally the interaction of two drops maintained at different temperatures and found that the drops exhibit non-coalescence behavior due to the presence of thermally induced Marangoni stresses above a critical temperature difference. This finding was also later verified in Refs. [28, 29] via numerical simulations. Most relevant here are the previous studies in Refs. [19, 30] on the coalescence of a drop on the free-surface of a pool of the same liquid maintained at a higher temperature than the drop. They observed that the drop floats longer with increasing the temperature difference between the drop and pool (ΔT). Considering silicone oils with different viscosities as the working fluids, Geri et al. [19] demonstrated that the residence time (t_r) scales as $\Delta T^{2/3}$. This phenomenon can be explained as follows, since the increase in residence time is due to the thermally induced Marangoni flow inside the drop which causes the air trapped between the drop and the pool to move inward instead of draining outward.

The Marangoni number (Ma) is a dimensionless number that characterizes the thermal convection owing to the surface tension gradient [31–33].

$$Ma = \left(\frac{d\sigma}{dT}\right)\frac{\Delta T D_p}{\mu_l \alpha}, \tag{1}$$

where D_p is the diameter of the primary drop, μ_l is the dynamic viscosity and α is the thermal diffusivity of the liquid. As increasing ΔT increases the Marangoni number, which enhances the internal circulation in the upward direction inside the drop. In order to balance this flow, the trapped air compressed inward, thereby maintaining the air cushion between the drop and the pool. However, for the Marangoni convection to develop, the residence time should be higher than the time scale of thermal diffusion ($t_c = {D_p}^2/\alpha$). This is the basic difference between the present study and the previous investigations [19, 30], who provided significant time for the development of Marangoni convection by anchoring the drop between the needle and free-surface, and the Faraday instabilities that allow the drop to float on the free-surface can also be observed. In contrast, in our experiments, as we allow the drop to fall freely from the needle onto the free-surface of the pool, the residence time is quite low as compared to the diffusion time scale. Ethanol is used as a working fluid. In addition, the size of the tank used in our study is sufficiently large so that the coalescence dynamics is free from the reflected waves from the boundaries.

In the present study, we revisit the coalescence dynamics of an ethanol drop (always at 25°C) slowly placed on the free-surface of an ethanol pool maintained at different temperatures (T_s) by conducting experiments using a high-speed camera. A parametric study is carried out by varying the diameter of the primary drop (D_p) released from a dispensing needle and the height of the needle tip from the ethanol-air interface (H) at different values of T_s. We observe complete coalescence without the formation of daughter droplet and partial coalescence depending on the parameters considered. A regime map designating the complete coalescence and partial coalescence dynamics is also plotted in $T_s - H$ space.

The rest of the paper is arranged as follows. The details of the experimental set-up and procedure followed are given in Section 2. The results obtained from our study are presented in Section 3 and the concluding remark is provided in Section 4.

2. Experimental set-up and procedure

We investigate experimentally the coalescence dynamics of ethanol drops that are slowly placed on the ethanol-air interface in a container (inner size 48 mm × 48 mm × 48 mm) filled with pure ethanol up to 15 mm. The ethanol in the container is maintained at different temperatures using a heater. Fig. 1 depicts the schematic diagram of the experimental set-up used in the present study. It consists of three main components, namely (i) an acrylic container with an aluminum metallic base placed on a heater, (ii) a droplet generation and dispensing system and (iii) a high-speed imaging and illumination system. The side-walls of the container is made up of an acrylic sheet (of thickness 4 mm) in order to provide optical access to the high-speed imaging system. Due to the high heat conductivity, an aluminum plate (of thickness of 12 mm) is used as the base of the container, which helps to maintain the ethanol in the container at various elevated temperatures. A sufficiently large container size is used, so that the reflected waves from the walls have negligible effects on the coalescence dynamics.

The temperature of the heater is varied and six values of the temperature of the ethanol-air interface in the pool (T_s), namely 25°C, 30°C, 35°C, 40°C, 45°C and 50°C, are considered. Fig. 2 shows the temperature variation inside the liquid pool. Here, $y = 0$ and $y = 15$ mm represent the top of the aluminum plate placed on the heater and the ethanol-air interface of the ethanol

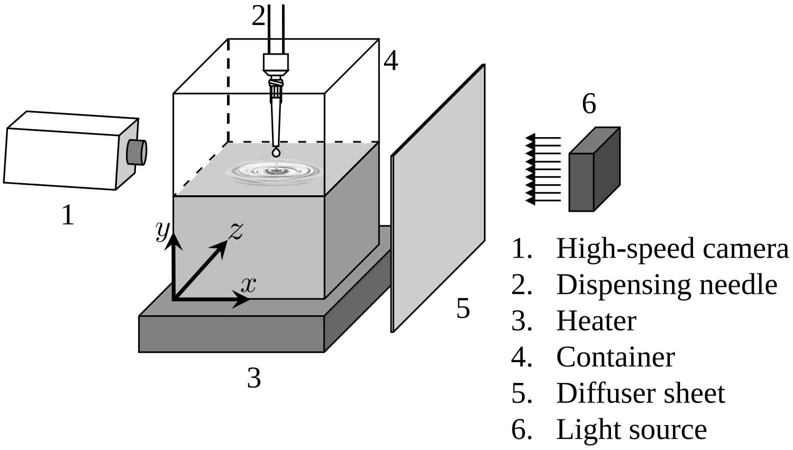

Figure 1: Schematic of the experimental set-up. It consists of a high-speed camera, a dispensing needle, a heater, an acrylic container with an aluminum metallic base, a diffuser sheet and a light source. The inner dimension of the container is 48 mm × 48 mm × 48 mm. The thickness of the acrylic side walls of the container is 4 mm and the thickness of the aluminum metallic base is 12 mm. The height of ethanol in the container is 15 mm.

pool, respectively. The heater temperature is fixed at a slightly higher value, T_s + 3°C, to keep the ethanol-air interface temperature at a particular value of T_s. The ethanol inside the container placed in the heater is stirred during the heating process to obtain the desired homogeneous temperature. After the desired interface temperature is reached, we stop stirring and measure the temperatures inside the ethanol pool at different heights (namely, y = 0 mm, 4 mm, 8 mm, 12 mm and 15 mm) using the K-type thermocouples. Fig. 2 presents the temperature variations in the vertical direction for different values of T_s. It is observed that temperature measurement uncertainty is about ±1.5°C that is associated with the thermocouple calibration error. The fluid properties of ethanol at different temperatures are listed in Table 1.

Table 1: The values of surface tension (σ), dynamic viscosity (μ_l) and density (ρ_l) of ethanol at different temperatures [34–36].

Temperature (°C)	σ (mN/m)	μ_l (mPa·s)	ρ_l (kg/m^3)
25	21.93	1.20	783.92
30	21.48	1.01	778.91
35	21.04	0.87	773.85
40	20.64	0.87	768.74
45	20.22	0.73	763.57
50	19.83	0.71	758.34

The droplet generation and dispensing system consists of a syringe pump (SP-810) fitted with different grades of blunt edge needle, namely 12 G, 14 G, 16 G, 18 G, and 20 G. This system is also facilitated by means of a traversing mechanism to anchor the needle height from the ethanol-air interface of the pool. By changing the ethanol volumetric flow rate and using different needles, we create different sizes of ethanol droplets at 25°C. The drops released from the needles come

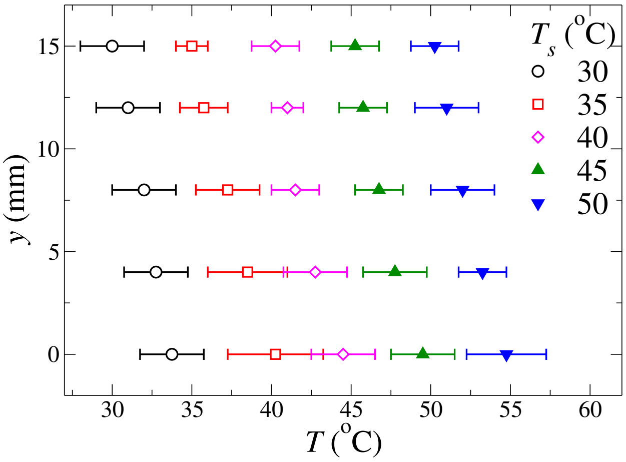

Figure 2: The temperature profiles in the ethanol pool for different values of ethanol-air interface temperature, T_s.

into contact with the ethanol pool kept at various temperatures. In our experiments, at the time of release, the distance between the bottom of the drops and the free-surface of the ethanol pool (h) is kept constant at 0.4 ± 0.05 mm, except when we examine the effect of the height the dispensing needle tip from the free-surface (H) on the coalescence dynamics.

A high-speed imaging and lighting system (shadowgraphy) consists of a Photron camera (Model - Fastcam SA1.1) along with a Nikon lens of 50 mm focal length is used to record the coalescence dynamics. The camera is kept at an angle of 7° to the horizontal as shown in Fig. 1 to visualize the droplet coalescence at the horizontal ethanol-air interface. A diffused backlit Light Emitting Diode (LED) illumination system (model 900445, 12000lm, Visual Instrumentation Corporation) is used to illuminate the test section of the transparent wall container. Images at a resolution of 320 × 240 pixels are recorded at a frame rate of 10000 frames per second (fps) with an exposure time of 10 μs. The recorded images are analyzed using the Matlab software. For each value of T_s, experiments are repeated 5 times to ensure repeatability. The reported uncertainty is estimated based on the standard deviation obtained from the five repetitions.

A droplet of ethanol placed slowly on the free-surface of the ethanol pool floats on the free-surface for some time (residence time, t_r), which depends on pool temperature (T_s) and the impact height (H) and the size of the primary droplet (D_p), before draining inside the ethanol pool. The comparison of the residence time and the thermal diffusion time scale is provided in Table 2 at T_s = 25°C (isothermal condition). It can be seen that in our experiment the residence time is much shorter than the time scale associated with thermal diffusion. In all our experiments, it is observed that the coalescence phenomenon occurs very quickly; the time taken for this process is always less than 75 ms. Thus, a freely falling drop does not get enough time to develop the Marangoni flow. This point has also been discussed in the introduction section. At later times, we also observe partial coalescence behavior for some set of parameters. In the following section, the coalescence dynamics of an ethanol drop observed for different sets of parameters are analyzed.

Table 2: Comparison of the thermal diffusion time scale ($t_c = {D_p}^2/\alpha$) and residence time (t_r) for different sizes of ethanol drop. The thermal diffusivity (α) of ethanol is 0.0827 mm^2/s.

D_p (mm)	t_c (s)	t_r (s)
1.71	35.3	0.063
1.83	40.5	0.043
2.05	50.8	0.030
2.10	53.3	0.025

3. Results and discussion

The primary objective of this study is to investigate the coalescence dynamics of an ethanol drop that is slowly placed in an ethanol-air interface in an ethanol pool maintained at different elevated temperatures (T_s). We also carried out a parametric study by varying the diameter of the primary drop (D_p) released from a dispensing needle and the height of the needle tip from the ethanol-air interface (H) at different values of T_s.

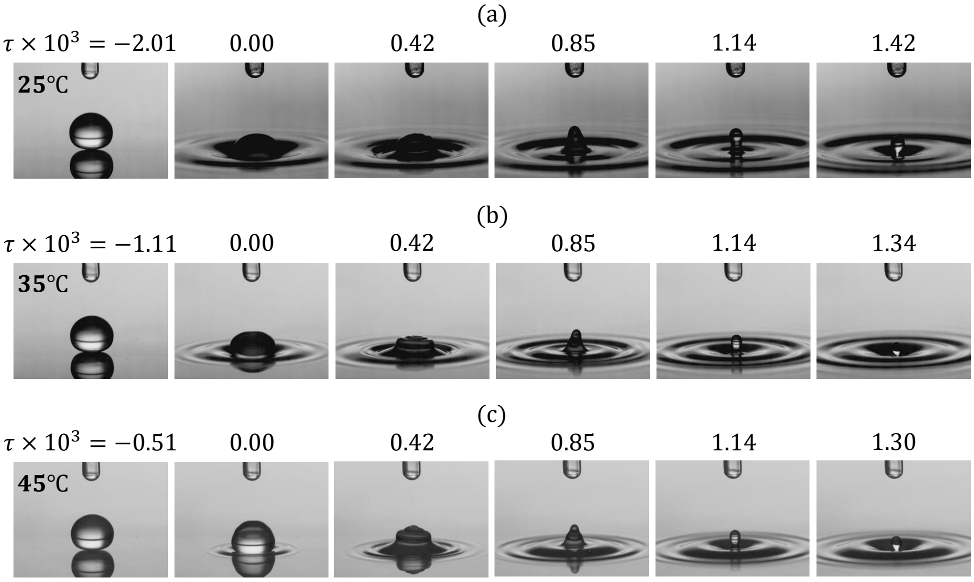

Figure 3: The temporal evolutions of the coalescence dynamics of an ethanol drop of diameter, $D_p = 1.83$ mm for different values of ethanol-air interface temperature in the pool, T_s. The dimensionless time, $\tau = t/t_c$ is written at the top of each image, such that $\tau = 0$ represents the instant when the drop starts draining in the liquid pool. Multimedia views: Multimedia 3a, 3b and 3c demonstrate the dynamics at T_s = 25°C (panel a), T_s = 45°C (panel b) and T_s = 55°C (panel c), respectively.

We begin the presentation of our results by analyzing the temporal evolutions of the coalescence dynamics of an ethanol drop of $D_p = 1.83$ mm at T_s = 25°C, 35°C and 45°C in Fig. 3. This figure demonstrates the topological changes that drop exhibits during the coalescence process when it is gently placed on the ethanol-air interface of the ethanol pool. The impact velocity (U) of the drop that is calculated using two consecutive frames of the drop just before it touches the interface is found to be very small (≈ 0.03 m/s). Note that in order to calculate the terminal velocity, the coordinates of the center of gravity of the drop in different instants are obtained and then the velocity (U) of the drop is calculated as $U = \Delta y/\Delta t$. Here, $\Delta y = y_n - y_{n-m}$, wherein y_n is the $y-$ coordinate of the drop's centre of gravity just before the it touches the free surface (say at frame 'n') and y_{n-m} is the location of the drop's centre of gravity at $n - m$ frame; Δt represents the time difference between these frames. We use $m = 20$ which corresponds to $\Delta t = 0.002$ s as the acquisition of the images is performed at 10000 frames per second, and Δy is the distance travel by the drop in Δt. Fig. 3(a) demonstrates the coalescence dynamics of an ethanol drop in an isothermal condition (Multimedia view 3a), i.e. when the drop and ethanol pool are at the same temperature (25°C). Figs. 3(b) and (c) show the coalescence dynamics of an ethanol drop in non-isothermal conditions, wherein the drop is at 25°C and the ethanol pool is at 35°C and 45°C, respectively (see Multimedia views 3b and 3c). The first column in panels (a-c) is associated with the instant at which the drop just touches the ethanol-air interface of the pool. The second column corresponds to the onset of the coalescence/draining of the drop inside the pool. The number written at the top of each image represents the dimensionless time, $\tau = t/t_c$. The time, t is calculated in such a way that dimensionless time, τ is zero at the onset of the coalescence, and the negative and positive values of τ represent the periods before and after the onset of coalescence, respectively. The temporal evolution of the drop dynamics is presented in the subsequent columns in Fig. 3. The first pinch-off of the daughter droplet (partial coalescence dynamics) is shown in the last panel for each value of T_s.

In the isothermal condition ($T_s = 25$°C), it can be seen in Fig. 3(a) that the dimensionless residence time of the drop is 2.01. During this period the drop floats on the ethanol-air interface in the pool until the air trapped between the drop and the free-surface is drained out. At $\tau = 0$, the drop starts to drain inside the pool and a neck is formed at the contact point of the drop and the free-surface, which expands rapidly due to high capillary pressure near the contact region (see, at $\tau = 0.42$; third column). Due to this, upward-moving capillary waves are generated, and thereby forming a liquid column (see, at $\tau = 0.85$; fourth column). This is followed by a necking process near the contact region (see, at $\tau = 1.14$; fifth column). Subsequently, the diameter of the neck is reduced due to the inward pull of the surface tension and a daughter droplet is detached (see, at $\tau = 1.42$; sixth column). This pinch-off of the daughter droplet occurs when the vertical collapse rate decreases due to the upward pull exerted by the capillary waves and thereby the horizontal collapse succeeds in merging the neck and producing a daughter droplet. The coalescence dynamics of a drop in the isothermal condition has been studied by several researchers (see, for instance, Refs. [11, 13, 14, 16, 17, 37, 38] as discussed in the introduction section).

A qualitatively similar coalescence dynamics is also observed in the non-isothermal cases presented in Fig. 3(b) and (c) for $T_s = 35$°C and 45°C, respectively. However, inspection of the dimensionless residence time and pinch-off time (defined as the difference between the instants at which the first pinch-off occurs and the onset of coalescence) decrease as the temperature of the ethanol pool increases. The dimensionless residence times of the drop for $T_s = 35$°C and 45°C are 1.11 and 0.51, respectively. It is to be noted that increasing the temperature decreases the surface tension, viscosity and density of ethanol [34–36]. As the ethanol drop at 25°C comes in contact with a hotter ethanol free-surface in the pool, the Marangoni convection starts to develop due to the gradient of surface tension resulting from the temperature gradient along the ethanol-air interface.

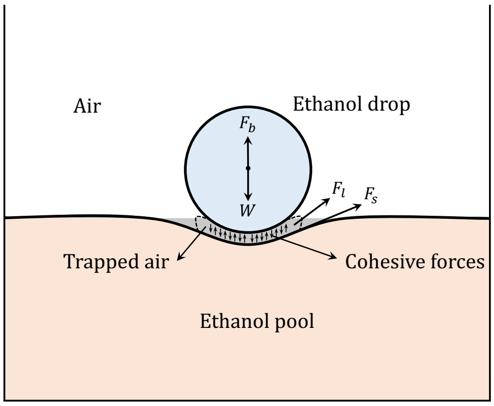

Figure 4: A sketch of different forces acting on a drop that is gently placed on the free-surface of a liquid pool. The various forces experienced by the drop are the weight of the drop (W), buoyancy force (F_b), surface tension force acting along the curved free-surface in the pool (F_l) and lift force due to the squeezed air (F_s).

Increasing the temperature of the ethanol pool increases this Marangoni convection. However, unlike Geri et al. [19], in our case due to the low residence time, the drop did not get sufficient time to develop the fully-developed Marangoni convection. The mechanism of the coalescence dynamics observed in our non-isothermal cases is discussed next.

In Fig. 4, we analyzed the forces acting on the drop when it floats at the free-surface of the ethanol pool to explain the decrease in the residence time with the increase in pool temperature. The weight of the drop creates a depression on the free-surface with an air film trapped in between the drop and ethanol-air interface in the pool. The various forces experienced by the drop during this time are the weight of the drop acting in the downward direction (W), upward buoyancy force (F_b), surface tension force acting along the curved free-surface in the pool ($F_l = 2\pi r_c \sigma$) and lift force due to the squeezed air which drains outward ($F_s = \rho_a v^2 A/2$). Here, ρ_a is the density of air, v is the velocity of squeezed out air, and A and r_c are the surface area and the radius of the curved surface, respectively. When the drop floats on the free-surface of the pool, the normal components of these forces acting on the drop balance each other. The surface tension delays coalescence by making the free-surface curve to accommodate the drop. Increasing temperature decreases the surface tension, which in turn decreases the free-surface depression. This is evident in Fig. 3 (second column), where it can be seen that at the onset of coalescence ($\tau = 0$), the radius of the curved free-surface in the isothermal case ($T_s = 25$°C) is significantly large (almost the same as the radius of the drop). It can be seen that the free-surface depression decreases with increasing the temperature of ethanol in the pool. At $T_s = 45$°C, the free-surface is almost flat at the onset of the coalescence. The decrease in the free-surface depression results in faster coalescence, i.e. decreases the residence time, t_r of the drop. At the later stage ($\tau \geq 0$), the drop touches the free-surface after draining the air cushion. The Marangoni convection from hotter to colder regions (i.e. in the upward direction) builds up once the drop touched the ethanol-air interface in the pool. Increasing the temperature gradient between the drop and ethanol pool increases the surface tension gradient, which in turn enhances the upward moving capillary waves due to Marangoni convection. As a consequence, increasing temperature reduces the rate of vertical collapse, resulting in faster daughter droplet formation (see Fig. 3) due to the more dominant horizontal collapse.

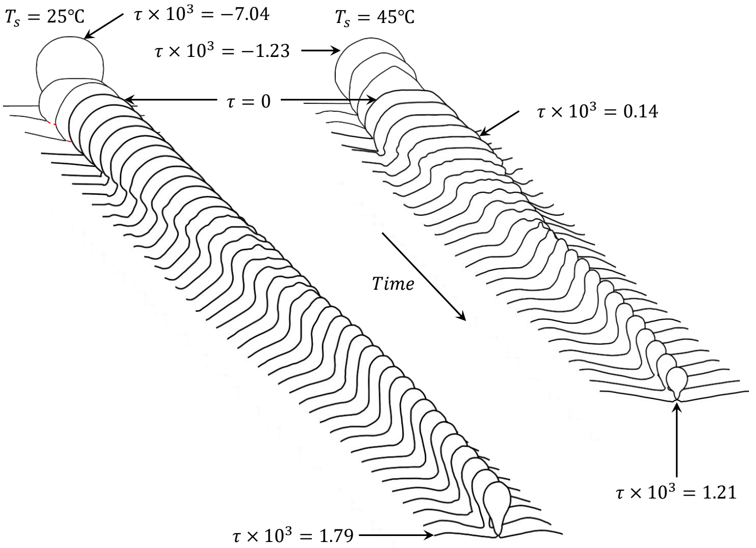

Figure 5: Temporal evolutions of drop profile at T_s = 25°C and 45°C. In both the cases, the diameter of the primary drop, $D_p = 1.71$ mm. The value of $\Delta\tau$ between two consecutive profiles after the drop touches the free-surface in the pool is 0.046×10^{-3}.

To gain more insight, in Fig. 5, we compare the temporal evolutions of drop profiles during the coalescence process at T_s = 25°C (isothermal case) and 45°C (non-isothermal case). In both cases, the drop diameter, D_p is kept constant at 1.71 mm. It can be seen that the drop is almost spherical in both cases when it is sufficiently away from the free-surface of the pool. Note that as the drop approaches the free-surface, it becomes difficult to obtain the distinct interfaces of the drop and free-surface from the image processing. It can be seen that for $\tau < 0$ the drop undergoes vertical oscillations, which is more in the isothermal case as compared to the non-isothermal case. These vertical oscillations in the drop try to regain the air cushion between the drop and the free-surface in the pool before the coalescence starts at $\tau = 0$. It can be seen in both cases that as the drop starts to drain inside the pool, the neck between the drop and the free-surface expands rapidly due to high capillary pressure near the contact region. In the isothermal case, due to the resultant upward-moving capillary waves, a vertical liquid column is created. As it grows the horizontal collapse due to the inward pull of the surface tension shrinks the neck region and a daughter droplet is created at $\tau = 1.79 \times 10^{-3}$. In Fig. 5, it can be seen at $\tau = 1.79 \times 10^{-3}$ and $\tau = 1.21 \times 10^{-3}$ for T_s = 25°C and 45°C that the interface of the drop and the pool form a sharp cone angle, after which blunting of this cone angle and capillary waves creeping on droplet surface are observed. This is the instant at which a daughter droplet is formed. The coalescence time is defined as the difference between the moment the capillary waves begin to ascend on the droplet surface due to the effect of Marangoni and the detachment of the daughter droplet. In contrast to the isothermal case, for T_s = 45°C, the drop spreads more on the free-surface in the pool during the draining stage. A significantly flat drop summit is observed at T_s = 45°C. In this case, the intensity of the upward moving capillary waves produced due to the expansion of the neck region between the drop and the free-surface are enhanced by the resultant Marangoni convection due

(a) Partial coalescence

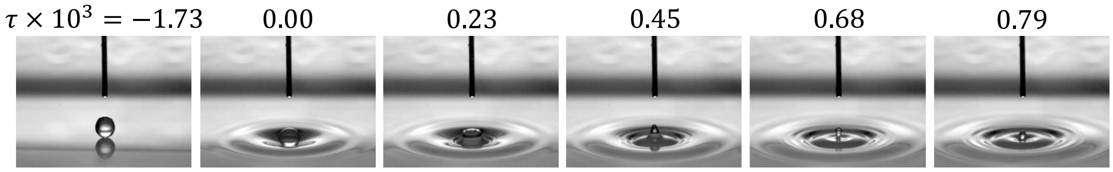

(b) No partial coalescence

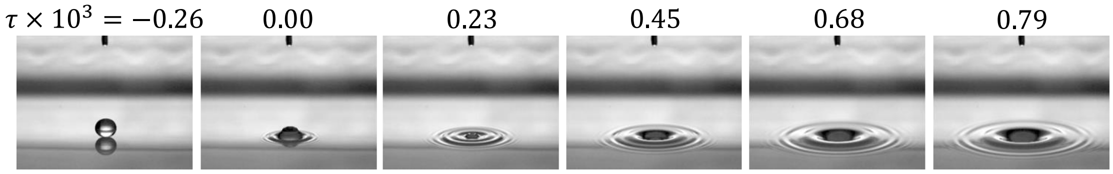

Figure 6: The effect of the height of the needle tip from the free-surface of the pool, H on the coalescence dynamics of an ethanol drop of primary diameter, D_p = 1.71 mm at T_s = 30°C. (a) H = 3.66 mm and (b) H = 7.83 mm. The value of the dimensionless time, τ is shown at the top of each panel. $\tau = 0$ represents the instant at the onset of coalescence. Multimedia views: Multimedia 6a and 6b demonstrate the dynamics at H = 3.66 mm (panel a) and H = 7.83 mm (panel b), respectively.

to the temperature gradient. This is evident after $\tau = 0.14 \times 10^{-3}$ for T_s = 45°C. This in turn prevents the column to drain into the pool and the neck region becomes thinner and detached from the free-surface of the pool due to the horizontal collapse at $\tau = 1.21 \times 10^{-3}$. Thus, the temperature gradient promotes the partial coalescence phenomenon.

Next, we investigate the effect of the height of the needle tip from the free-surface of the pool (H) on the coalescence dynamics of a drop of D_p = 1.71 mm in Fig. 6. Figs. 6(a) and (b) present the dynamics for H = 3.66 mm and H = 7.83 mm, respectively. The dynamics for H = 3.66 mm and H = 7.83 mm are also presented as Multimedia views 6a and 6b, respectively. The first and second columns in each panel represent the frames when the drop touches the free-surface and starts to coalesce in the pool, respectively. The columns that follow demonstrate the dynamics as the time progresses. Increasing H increases the potential energy of the drop, which is converted into kinetic energy, and thereby increasing the impact velocity of the drop falling into the ethanol pool. The value of the impact velocities of the drop for H = 3.66 mm and H = 7.83 mm are 0.12 m/s and 0.32 m/s, respectively. It can be seen that the drop floats on the free-surface for longer time ($\tau = 1.73$) for H = 3.66 mm, as compared to H = 7.83 mm. The drop also demonstrates the partial coalescence phenomenon at $\tau = 0.79$ for H = 3.66 mm, whereas this behavior does not occur for H = 7.83 mm and the drop completely coalesce inside the pool creating a much bigger depression on the free-surface at the same dimensionless time. Close inspection of Figs. 6(a) and (b) also reveals that increasing the impact velocity decreases with the width of the crater developed at the interface. It indicates that in the case of a drop with a high impact velocity, the upward force to support the drop becomes insignificant as compared to a gently placed drop with a negligible impact velocity. Increasing the impact velocity of the drop significantly decreases the vertical component of the surface tension force and also decreases the buoyant force as the swept volume is displaced farther away. Complete coalescence is observed in the case of a high impact velocity drop. Thus, as expected, it can be inferred that in addition to the fluid properties, the

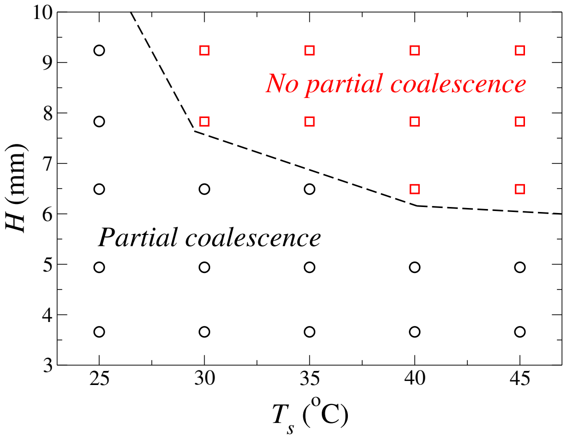

Figure 7: Regime map showing the partial coalescence and complete coalescence without forming a daughter droplet in T_s - H space. Here, the diameter of the primary drop, D_p = 1.71.

needle height also plays an important role in the coalescence dynamics.

In Fig. 7, we present the regimes associated with the partial coalescence (black circles) and complete coalescence without the formation of a daughter droplet (red squares) in T_s - H space for a primary drop of size, $D_p = 1.71$ mm. To ensure repeatability, experiments are performed five times for each set of values of T_s and H. It can be seen that in the isothermal condition ($T_s = 25$°C), the partial coalescence phenomenon is observed for all H values considered in the present study. For $T_s \geq 30$°C, the partial coalescence phenomenon is only observed for low values of H. This is due to the competition between the upward moving capillary waves and the impact velocity of the drop. In other words, increasing the momentum force generated by a falling droplet (i.e., increasing the height of the nozzle) decreases the intensity of the upward moving capillary waves which allows the drop to penetrate into the pool leading to complete coalescence. It can be seen that the critical value of H at which the drop changes its behavior from partial coalescence to complete coalescence decreases with increasing temperature of the ethanol pool.

Then we conduct a parametric study by varying the diameter of the primary drop injected from the needle (D_p) and ethanol pool temperature, T_s. The height of the bottom of the drop from the free-surface is fixed at $h = 0.4 \pm 0.05$ mm. The parameters are chosen in such a way that the drop exhibits partial coalescence for all values of T_s. In Fig. 8, we present the variations in the diameter of the daughter droplet (D_s) obtained for different sizes of the primary drop (D_p) at different values of T_s. Five primary drop sizes (i.e. D_p =1.71 mm, 1.83 mm, 1.96 mm, 2.05 mm and 2.10 mm) and four values of T_s (i.e. T_s = 25°C, 30°C, 40°C and 45°C) have been considered to generate this plot. It can be seen that increasing temperature decreases the size of the daughter droplet for all sizes of the primary drop considered. This is because, as discussed above, increasing temperature promotes the drainage of the primary drop, thereby leaving a smaller volume of ethanol in the column for the daughter droplet creation. It can be observed that increasing D_p decreases the size of the daughter droplet to an asymptotic value. Inspection of this figure also reveals that D_s/D_p is about 0.5 for $D_p = 1.71$ mm in the isothermal condition, which is similar to the value observed in the previous studies [14, 17].

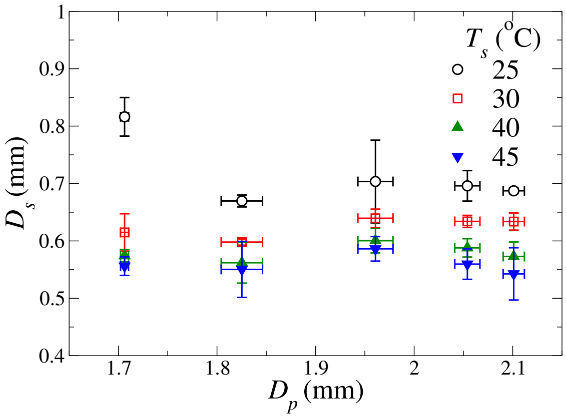

Figure 8: Variations of the diameter of the first daughter droplet (D_s in mm) with the diameter of the primary drop (D_p in mm) for different values of T_s.

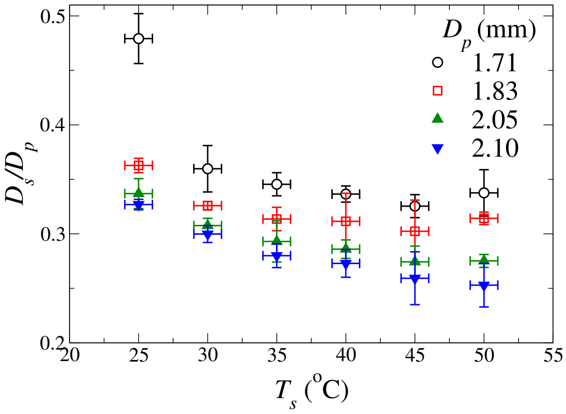

Figure 9: The variations of D_s/D_p with T_s for different values of primary diameter of the ethanol drop, D_p.

Fig. 9 shows the variations of D_s/D_p with T_s for different values of D_p. It can be seen that increasing the pool temperature, T_s decreased the value of D_s/D_p for all sizes of the primary drop. In all the cases, the value of D_s/D_p is less than 0.5. Close inspection of Fig. 8 and Fig. 9 also reveals that increasing the size of the primary drop decreases the values of D_s/D_p for all values of T_s considered. In isothermal system, Chen et al. [14] also showed that the drop goes from the inertio-capillary regime to the gravity regime and thereby, decreasing the value of D_s/D_p as we increase the size of the primary drop.

Finally, the variations of the dimensionless residence time, τ_r with the free-surface temperature of the pool, T_s are presented for different values of D_p and H in Fig. 10(a) and (b), respectively. It can be seen in Fig. 10(a) that increasing the temperature of the ethanol pool decreases the residence time for all values of D_p. Increasing D_p increased the weight of the drop, which promotes the draining of the trapped air in between the drop and the free-surface of the pool. Increasing the temperature of the pool decreases the surface tension and thus the free-surface could not become curve to hold the drop and coalescence starts. Thus increasing temperature decreases the residence time of the drop (see Fig. 10(b)). It can also be seen in Fig. 10(b) that as increasing height increases

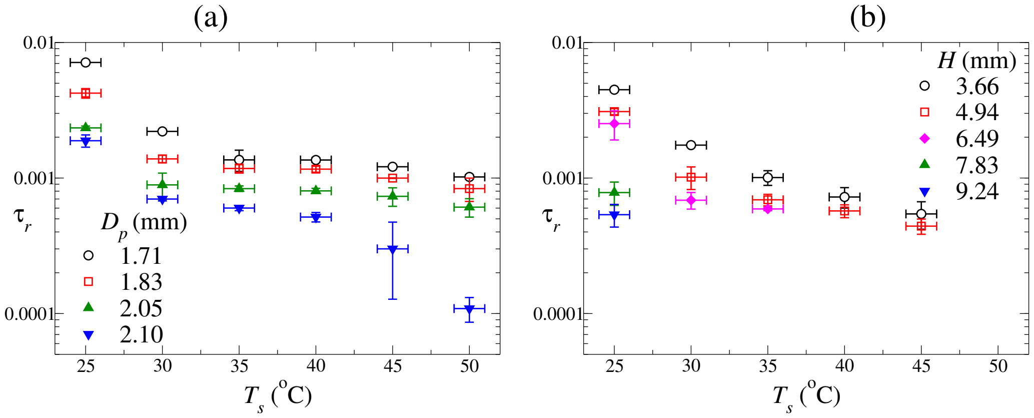

Figure 10: Variations of dimensionless residence time, $\tau_r = t_r/t_c$ with the temperature at the free-surface the ethanol pool, T_s for different values of (a) the diameter of the primary drop, D_p when the tip of the drop is at 0.4±0.05 mm from the free-surface, and (b) height of the needle tip from the ethanol-air interface, H for $D_p = 1.83$ mm.

the impact velocity of the drop, which drains the trapped air easily and reduces the residence time.

4. Concluding remarks

In this study, we revisit the coalescence dynamics of a drop (at 25°C) slowly placed on the free-surface of a pool maintained at different temperatures (T_s) by conducting experiments. The experimental set-up consists of a high-speed camera, a dispensing needle, a heater, an acrylic container of inner dimension 48 mm × 48 mm × 48 mm with an aluminum metallic base, a diffuser sheet and a light source. The container is filled with ethanol to a height of up to 15 mm. It is observed that the ethanol drop exhibits a residence phase, when it floats on the free-surface before the coalescence begins. Subsequently, the complete coalescence and partial coalescence dynamics are observed for different sets of parameters considered. In our experiments as we considered the coalescence of a freely falling drop, the residence time is much shorter than the time scale associated with thermal diffusion. Thus, drop does not get enough time to develop the Marangoni flow during the residence phase, which was found to play a key role in delaying the coalescence in the previous studies [19, 30].

We carried out a parametric study by varying the diameter of the primary drop (D_p) released from a dispensing needle and the height of the needle tip from the ethanol-air interface (H) at different values of T_s. It is found that increasing the temperature of the ethanol pool reduces the residence time of the drop. This phenomenon is explained by analyzing the forces acting on the drop and the capillary waves generated due to the temperature gradient between the drop and the ethanol pool. As expected, due to the gravity effect, increasing the size of the primary drop also decreases the residence time. The partial coalescence phenomenon is observed for low impact height and it is found that the diameter of the daughter droplet decreases as the size of the primary drop and pool temperature are increased. A regime map designating the complete coalescence and partial coalescence dynamics is plotted in $T_s - H$ space.

Data Availability Statement:

The data that support the findings of this study are available from the corresponding author upon reasonable request.

Acknowledgement

K. C. S. and P. K. thank the Science & Engineering Research Board, India for their financial support (Grant numbers: MTR/2017/000029 and ECR/2015/000365).

[1] H. A. Stone, A. D. Stroock, A. Ajdari, Engineering flows in small devices: microfluidics toward a lab-on-a-chip, Annu. Rev. Fluid Mech. 36 (2004) 381–411.

[2] S. T. Thoroddsen, T. G. Etoh, K. Takehara, High-speed imaging of drops and bubbles, Annu. Rev. Fluid Mech. 40 (2008) 257–285.

[3] F. H. Zhang, M. J. Thoraval, S. T. Thoroddsen, P. Taborek, Partial coalescence from bubbles to drops, J. Fluid Mech. 782 (2015) 209–239.

[4] K. Haldar, S. Chakraborty, Investigation of chemical reaction during sodium alginate drop impact on calcium chloride film, Phys. Fluids 31 (7) (2019) 072102.

[5] M. Kumar, R. Bhardwaj, K. C. Sahu, Coalescence dynamics of a droplet on a sessile droplet, Phys. Fluids 32 (1) (2020) 012104.

[6] R. Abdelaziz, D. Disci-Zayed, M. K. Hedayati, J. H. Pöhls, A. U. Zillohu, B. Erkartal, V. S. K. Chakravadhanula, V. Duppel, L. Kienle, M. Elbahri, Green chemistry and nanofabrication in a levitated leidenfrost drop, Nature Communications 4 (2013) 2400.

[7] B. Schwenzer, Leidenfrost drops prove to be versatile nanoreactors, MRS Bulletin 39 (1) (2014) 7–7.

[8] M. Mrinal, X. Wang, C. Luo, Self-rotation-induced propulsion of a leidenfrost drop on a ratchet, Langmuir 33 (25) (2017) 6307–6313.

[9] E. Mogilevskiy, Levitation of a nonboiling droplet over hot liquid bath, Phys. Fluids 32 (1) (2020) 012114.

[10] B. Ray, G. Biswas, A. Sharma, Regimes during liquid drop impact on a liquid pool, J. Fluid Mech. 768 (2015) 492–523.

[11] G. E. Charles, S. G. Mason, The mechanism of partial coalescence of liquid drops at liquid/liquid interfaces, J. Colloid Sci. 15 (2) (1960) 105–122.

[12] S. T. Thoroddsen, K. Takehara, The coalescence cascade of a drop, Phys. Fluids 12 (6) (2000) 1265–1267.

[13] H. Aryafar, H. P. Kavehpour, Drop coalescence through planar surfaces, Phys. Fluids 18 (7) (2006) 072105.

[14] X. Chen, S. Mandre, J. J. Feng, Partial coalescence between a drop and a liquid-liquid interface, Phys. Fluids 18 (5) (2006) 051705.

[15] X. Chen, S. Mandre, J. J. Feng, An experimental study of the coalescence between a drop and an interface in Newtonian and polymeric liquids, Phys. Fluids 18 (2006) 092103.

[16] F. Blanchette, T. P. Bigioni, Partial coalescence of drops at liquid interfaces, Nat. Phys. 2 (4) (2006) 254.

[17] B. Ray, G. Biswas, A. Sharma, Generation of secondary droplets in coalescence of a drop at a liquid–liquid interface, J. Fluid Mech. 655 (2010) 72–104.

[18] H. Deka, G. Biswas, K. C. Sahu, Y. Kulkarni, A. Dalal, Coalescence dynamics of a compound drop on a deep liquid pool, J. Fluid Mech. 866 (2019) R2 1–11.

[19] M. Geri, B. Keshavarz, G. H. McKinley, J. W. M. Bush, Thermal delay of drop coalescence, J. Fluid Mech. 833 (2017) R3.

[20] J. J. Thomson, H. F. Newall, On the formation of vortex rings by drops falling into liquids, and some allied phenomena, Proc. Royal Soc. Lond. 39 (239-241) (1886) 417–436.

[21] E. G. Cockbain, T. S. McRoberts, The stability of elementary emulsion drops and emulsions, J. Colloid Interface Sci. 8 (4) (1953) 440–451.

[22] A. Gopinath, D. L. Koch, Collision and rebound of small droplets in an incompressible continuum gas, J. Fluid Mech. 454 (2002) 145–201.

[23] Y. Couder, E. Fort, C. H. Gautier, A. Boudaoud, From bouncing to floating: Noncoalescence of drops on a fluid bath, Phys. Rev. Lett. 94 (17) (2005) 177801.

[24] K. Haldar, S. Chakraborty, S. Chakraborty, Influence of marangoni stress on the variation in number of coalescence cascade stages, Can. J. Chem. Eng. 97 (4) (2019) 983–994.

[25] P. Dell'Aversana, J. R. Banavar, J. Koplik, Suppression of coalescence by shear and temperature gradients, Phys. Fluids 8 (1) (1996) 15–28.

[26] P. Dell'Aversana, V. Tontodonato, L. Carotenuto, Suppression of coalescence and of wetting: The shape of the interstitial film, Phys. Fluids 9 (9) (1997) 2475–2485.

[27] P. Dell'Aversana, G. P. Neitzel, When liquids stay dry., Physics today 51 (1) (1998) 38–41.

[28] R. Monti, R. Savino, Correlation between experimental results and numerical solutions of the navier–stokes problem for noncoalescing liquid drops with marangoni effects, Phys. Fluids 9 (2) (1997) 260–262.

[29] R. Monti, R. Savino, A. Cicala, Surface tension driven-flow in non-coalescing liquid drops, Acta Astronautica 38 (12) (1996) 937–946.

[30] R. Savino, D. Paterna, M. Lappa, Marangoni flotation of liquid droplets, J. Fluid Mech. 479 (2003) 307–326.

[31] M. F. Schatz, G. P. Neitzel, Experiments on thermocapillary instabilities, Annu. Rev. Fluid Mech. 33 (1) (2001) 93–127.

[32] M. Balla, M. K. Tripathi, K. C. Sahu, G. Karapetsas, O. K. Matar, Non-isothermal bubble rise dynamics in a self-rewetting fluid: three-dimensional effects, J. Fluid Mech. 858 (2019) 689–713.

[33] M. K. Tripathi, K. C. Sahu, G. Karapetsas, K. Sefiane, O. K. Matar, Non-isothermal bubble rise: non-monotonic dependence of surface tension on temperature, J. Fluid Mech. 763 (2015) 82–108.

[34] G. Vazquez, E. Alvarez, J. M. Navaza, Surface tension of alcohol + water from 20 to 50°c, J. Chem. Eng. Data. 40 (3) (1995) 611–614.

[35] V. F. Nozdrev, The viscosities of ethanol-cyclohexane mixtures, Zh. Fiz. Khim. 49 (1975) 548–549.

[36] I. F. Golubev, T. N. Vasil'Kovskaya, V. S. Zolin, Experimental study of the density of aliphatic alcohols at various temperatures and pressures, J. Eng. Phys. 38 (4) (1980) 399–401.

[37] T. Dong, W. H. Weheliye, P. Chausset, P. Angeli, An experimental study on the drop/interface partial coalescence with surfactants, Phys. Fluids 29 (10) (2017) 102101.

[38] H. Ma, C. Liu, X. Li, and H. Huang, and J. Dong, Deformation characteristics and energy conversion during droplet impact on a water surface, Phys. Fluids 31 (6) (2019) 062108.